



HAL
open science

Exotic atoms

Paul Indelicato

► **To cite this version:**

| Paul Indelicato. Exotic atoms. Physica Scripta, 2004, T112, pp.20-26. hal-00002825

HAL Id: hal-00002825

<https://hal.science/hal-00002825>

Submitted on 11 Sep 2004

HAL is a multi-disciplinary open access archive for the deposit and dissemination of scientific research documents, whether they are published or not. The documents may come from teaching and research institutions in France or abroad, or from public or private research centers.

L'archive ouverte pluridisciplinaire **HAL**, est destinée au dépôt et à la diffusion de documents scientifiques de niveau recherche, publiés ou non, émanant des établissements d'enseignement et de recherche français ou étrangers, des laboratoires publics ou privés.

Exotic atoms

Paul Indelicato^{1,*},

¹ Laboratoire Kastler-Brossel, École Normale Supérieure et Université P. et M. Curie, Case 74, 4 place
Jussieu, F-75252, Cedex 05, France

Abstract

In this paper I review a number of recent results in the field of exotic atoms. Recent experiments or ongoing experiments with muonic, pionic and antiprotonic hydrogen, as well as recent measurement of the pion mass are described. These experiments provide information about nucleon-pion or nucleon-antinucleon interaction as well as information on the proton structure (charge or magnetic moment distribution).

PACS numbers: 06.20.Fn, 32.30.Rj, 36.10.-k, 07.85.Nc

ccsd-00002825, version 1 - 12 Sep 2004

*Email address: paul.indelicato@spectro.jussieu.fr

1 Introduction

Exotic atoms are atoms that have captured a long-lived, heavy particle. This particle can be a lepton, sensitive only to the electromagnetic and weak interactions, like the electron or the muon, or a meson like the pion, or a baryon like the antiproton. An other kind of exotic atom is the one in which the *nucleus* has been replaced by a positron (positronium, an e^+e^- bound system) or a positively charged muon (muonium, a μ^+e^- bound system). Positronium and muonium are pure quantum electrodynamics (QED) systems as they are made of elementary, point-like Dirac particles insensitive to the strong interaction. The annihilation of positronium has been a benchmark of bound-state QED (BSQED) for many years. For a long time there has been an outstanding discrepancy between the calculated (see, e.g., [1] for a recent review) and measured lifetime of ortho-positronium in vacuum, that has been resolved recently [2]. As the positronium is the best QED test system, such a discrepancy was considered very serious. The $1^3S_1 \rightarrow 2^3S_1$ transition has also been measured accurately [3].

Muonium has also been investigated in detail (see e.g., [4].) Both the ground state hyperfine structure [5] and the $1s \rightarrow 2s$ transition [6, 7, 8, 9] have been investigated theoretically [10, 11, 12] and experimentally. The work on the hyperfine structure provides a very accurate muon mass value as well as a value for the fine structure constant (see the CODATA recommended values of the fundamental constants [13]).

The capture of a negatively charged, heavy particle X^- by an atom, occurs at a principal quantum number $n \approx n_e \sqrt{\frac{m_X}{m_e}}$ where n_e is the principal quantum number of the atom outer shell, and m_e, m_X are respectively the electron and particle mass. This leads to $n = 14, 16$ and 41 for muons, pions and antiprotons respectively. The capture process populates ℓ sub-states more or less statistically. During the capture process of an heavy, negatively charged particle, many or all of the electrons of the initial atoms are ejected by Auger effect. As long as electrons are present, Auger transition rates are very large and photon emission is mostly suppressed except for the low lying states. For light elements, or particles like the antiproton, the cascade can end up with an hydrogenlike ion, with only the exotic particle bound to the nucleus [14].

The spectroscopy of exotic atoms has been used as a tool for the study of particles and fundamental properties for a long time. Exotic atoms are also interesting objects as they enable to probe aspects of atomic structure that are quantitatively different from what can be studied in electronic or “normal” atoms. For example, all captured particles are much heavier than the electron, and thus closer to the nucleus, leading to a domination of vacuum polarization effects over self-energy contributions, in contrast to normal atoms. The different relevant scales, Coulomb and vacuum polarization potential, together with pionic and electronic densities in pionic and normal hydrogen are represented on Fig. 1. One can see that the pion density inside the nucleus, or where the vacuum polarization potential is large, is several orders of magnitude larger than the electronic density in hydrogen. This leads to very large vacuum polarization and finite nuclear size corrections.

Other fundamental changes can be found in exotic atoms: pions are bosons, and thus obey the Klein-Gordon equation, while electrons, muons and antiprotons as spin 1/2 fermions, obey the Dirac equation.

Yet antiprotons, which are not elementary particles, have a magnetic moment very different from the one of a Dirac particle. This leads to large corrections not present in other types of atoms.

In the present paper, I will review a number of systems of interest for the study of the proton structure or of the strong interaction at low energy. In Section 2, I describe an ongoing experiment to measure the 2s Lamb-shift of muonic hydrogen. In section 3, I present recent experiments involving pionic atoms. Finally in section 4, I will review recent work on antiprotonic hydrogen and helium.

2 Muonic hydrogen and the determination of the proton charge radius

In the last decade very important progress has been made in the accuracy of optical measurements in hydrogen. With the help of frequency combs and rubidium fountain atomic clocks, the accuracy of the 1s→2s transition measurement has reached 1.8×10^{-14} , giving 2 466 061 413 187 103(46) Hz [15]. The Rydberg constant (which requires knowledge of e.g., 2s→nd transitions) that is needed to extract the Lamb-shift from the 1s→2s transition energy and to get theoretical values is now known to 7.7×10^{-12} [16]. From this information one can obtain the 1s and 2s Lamb-shift to 2.7 ppm accuracy. However for many years it has been impossible to use those very accurate measurements to test QED in hydrogen, which is the only atom, at the present moment, in which experimental uncertainty is much smaller than the size of two-loop BSQED corrections. Because in hydrogen $Z\alpha \ll 1$, calculations of radiative corrections have been done as an expansion in $Z\alpha$, i.e., expanding the electron propagator in the number of interaction with the nucleus. It is only recently that for the one-loop self-energy an exact, all order calculation, with a numerical precision small compared to the 46 Hz experimental error bar has been performed. For the two-loop self-energy, the situation is very complex. In the first calculation of the irreducible contribution to the loop-after-loop contribution (Fig. 2 a) it was found that the all-order contribution did not match, even at $Z = 1$, the result obtained by summing up all know term in the $Z\alpha$ expansion [17, 18]. This results was latter confirmed [19]. It should be noted that this piece has no meaning by itself, not being a renormalizable, gauge invariant set of Feynman graphs.

More recently the complete all-order two-loop self-energy has been evaluated, but only for $Z \geq 40$ [20]. It cannot be said at the moment wether the extrapolation to $Z = 1$ agrees with the $Z\alpha$ expansion (Fig. 3).

Yet the issue cannot be resolved with the help of experiment, as the proton charge radius is not well known, and the uncertainty on the theoretical value due to that fact is larger than any uncertainty on the two-loop corrections. Values of the proton radius measured by electron scattering range from 0.805(12) fm[21] to 0.847(11) [22] and 0.880(15) fm [23], the two later values resulting from reanalysis of the same experiment[24]. On the other hand, one obtains 0.908 fm from a comparison between measurements in hydrogen and QED calculation[13].

Owing to this large dispersion of results, the uncertainty in QED calculations is 4 times larger than the present experimental accuracy. It has thus been proposed to use muonic hydrogen to obtain an independent measurement of the proton radius. The experiment consists in measuring the 2s→2p_{3/2} transition energy, which is strongly dependent in the proton radius. From value of [12] for the “light by light” contribution

one gets

$$206.099(20) - 5.2256r^2 + 0.0363r^3 \text{ meV}, \quad (1)$$

where the number in parenthesis represent the uncertainty (quadratic sum), and where r , the proton mean spherical charge radius, must be expressed in Fermi. If one uses instead Ref. [25, 26], then one obtains 206.074(3) meV for the constant term.

An experiment aiming at an accuracy of 40 ppm of the $2s \rightarrow 2p_{3/2}$ energy difference has been started at the Paul Scherrer Institute (PSI). Such an accuracy would provide a proton charge radius to $\approx 0.1\%$ accuracy, which would allow to compare theory and experiment for the $1s$ and $2s$ Lamb-shift on hydrogen to the 0.4 ppm level. The experiment uses the fact that the $2s$ state is metastable in muonic hydrogen. This is due to the fact that, the muon being 206 times more massive than the electron (and thus 200 times closer to the nucleus), vacuum polarization dominates radiative corrections in exotic atoms, and has opposite sign compare to self-energy. The $2s$ state is thus the lowest $n = 2$ level in muonic hydrogen, while it is $2p_{1/2}$ in hydrogen. The experiment thus consists in exciting the $6 \mu\text{m } 2^3S_{1/2} \rightarrow 2^5P_{3/2}$ transition with a laser, and detects the 2 keV X-rays resulting from the $2p_{3/2} \rightarrow 1s$ transition that follows. In order to reduce background events, coincidence between the high-energy electrons resulting from the muon disintegration and the 2 keV X-rays must be done.

The experiment uses slow muons prepared in the *cyclotron trap II* [27], installed on the high-intensity pion beam at PSI. The muons, originating in pion decays, are decelerated to eV energies through interaction with thin foils inside the trap. They are then accelerated to a few keV, and transferred to a low density hydrogen target in a 5 T magnetic field, using a bent magnetic channel, to get rid of unwanted particles[28, 29]. A stack of foils at the entrance of the target is used to trigger an excimer laser in around $1 \mu\text{s}$ (the muons half life is around $2 \mu\text{s}$). This laser is at the top of a laser chain that use dye lasers, Ti-sapphire lasers and a multipass Raman cell filled with 15 bars of H_2 to produce the $6 \mu\text{m}$ radiation. The laser system is shown on Fig. 4. More details on the population of metastable states and on the experimental set-up as can be found in [30, 31, 32]. A first run of the experiment took place in summer 2002, in which an intensity of 0.3 mJ was obtained at $6 \mu\text{m}$, which is enough to saturate the transition, and ≈ 50 muons/h were detected in the target. Counting rate is expected to be around 5 events/h at the transition peak, which makes the experiment extremely difficult, owing to the uncertainty on where to look for the transition, and of the complexity of the apparatus.

3 Pionic atoms

Pions are mesons, i.e., particles made of a quark-antiquark pair. They are sensitive to strong interaction. To a large extent, the strong interaction between nucleons in atomic nuclei results from pion exchange. The lifetime of the charged pion is 2.8×10^{-8} s. They decay into a muon and a muonic neutrino. The mass of the pion is 273 times larger than the electron mass. Contrary to the electron, it has a charge radius of 0.8 fm and it is a spin-0 boson.

3.1 Measurement of the pion mass

For a long time the spectroscopy of pionic atoms has been the favored way of measuring accurately the pion mass. This mass was measured in 1986 in pionic magnesium, with a crystal X-ray spectrometer, to a 3 ppm accuracy [33, 34]. Yet, as the pions were stopped in solid magnesium, in which it was possible for the pionic atom to recapture electrons before de-excitation, it was found that the hypothesis made by Jeckelmann *et al.* on the number of electron recaptured in the atom was incorrect (in the pion cascade leading to the formation of the pionic atom, all the electron are ejected by auger effect.) This happened in experiments designed to measure the muonic neutrino mass, from the decay of stopped positively charged pions into muon and muonic neutrino [35]. This experiment found a negative value for the square of the neutrino mass, using the 1986 value of the pion mass. A reanalysis of the 1986 experiment, with better modeling of the electron capture was done, which lead to a pion mass value in agreement compatible with a positive value for the square of the neutrino mass.

Such a situation was very unsatisfactory and it was decided to use the cyclotron trap and the high-luminosity X-ray spectrometer, developed initially for work with antiprotons at the Low Energy Antiproton Ring (LEAR) at CERN to redo a measurement of the pion mass, in a low pressure gas, in which case electron recapture is negligible small. Moreover the resolution of the spectrometer was such that line resulting from the decay of an exotic atom with an extra electron would be separated from the main transition in a purely hydrogenlike exotic atom. In a first experiment a value from the pion mass was obtained by doing a measurement in pionic nitrogen, using copper $K\alpha$ X-rays as a reference [36]. This measurement, with an accuracy of 4 ppm, and in good agreement with the limits set by [35], allowed to settle the question of the pion mass. However the 4 ppm accuracy is not good enough for recent projects involving pionic hydrogen, which are discussed in Sec. 3.2. The schematic of the experiment is shown in Fig. 5.

The previous experiment accuracy was limited by the beam intensity, the characteristics of the cyclotron trap, the quality of the X-ray standard (broad line observed in second order of diffraction, while the pion line was observed in first order) and the CCD size and operation. It was decided to use the $5g \rightarrow 4f$ transition in *muonic* oxygen transition as a standard, with an energy close to the one of the $5g \rightarrow 4f$ transition in pionic nitrogen in place of the Cu energy standard, relying on the fact that the muon mass is well known [13]. This standard energy can be evaluated with a uncertainty of ≈ 0.3 ppm. A new trap was designed, optimized for muon production, which was also to be used for the experiment presented in Sec. 2. Meanwhile the beam intensity of the PSI accelerator had improved. Finally a new CCD detector was designed, with larger size, higher efficiency and improved operations [37].

With these improvements, a new experiment was done, which lead to a statistical accuracy in the comparison between the pionic and muonic line, compatible with a final uncertainty around 1 ppm [38]. However at that accuracy, effects due to the fabrication process of the CCD are no longer negligible and require very delicate study, e.g., to measure the pixel size. Those studies are underway.

A byproduct of the pion mass measurement has been a very accurate measurement of the $5 \rightarrow 4$ transition fine structure in pionic nitrogen. The energy difference between $5g \rightarrow 4f$ and $5f \rightarrow 4d$ is found to be 2.3082 ± 0.0097 eV [36], while a calculation based on the Klein-Gordon equation, with all vacuum polariza-

tion corrections of order α and α^2 and recoil corrections provides 2.3129 eV [39]. This is one of the best test of QED for spin-0 boson so far.

3.2 Pionic hydrogen and deuterium

Quantum Chromodynamics is the theory of quarks and gluons, that describe the strong interaction at a fundamental level, in the Standard Model. It has been studied extensively at high-energy, in the asymptotic freedom regime, in which perturbation theory in the coupling constant can be used. At low energy the QCD coupling constant α_S is larger than one and perturbative expansion in α_S cannot be done. Weinberg proposed Chiral Perturbation Theory (ChPT) [40] to deal with this problem. More advanced calculations have been performed since then, that require adequate testing. Short of the possibility of studying pionium (a bound pion-antipion system) accurately enough, pionic hydrogen is the best candidate for accurate test of ChPT. The shift and width of $np \rightarrow 1s$ transition in pionic hydrogen due to strong interaction can be connected respectively to the $\pi^-p \rightarrow \pi^-p$ and $\pi^-p \rightarrow \pi^0n$ cross-sections, which can be evaluated by ChPT, using a Deser-type formula[41]. After a successful attempt at studying pionic deuterium with the apparatus described in Sec. 3.1, which provided in a very short time a sizable improvement over previous experiments [42], it was decided that such an apparatus could lead to improvements in pionic hydrogen of a factor 3 in the accuracy of the shift and of one order of magnitude in the accuracy of the width. In order to reach such an improvement, systematic studies as a function of target density and of the transition ($np \rightarrow 1s$, with $n=2, 3$ and 4) have been done.

The main difficulty in the experiment is to separate the strong interaction broadening of the pionic hydrogen lines, from other contributions, namely the instrumental response function, Doppler broadening due to non-radiative de-excitation of pionic hydrogen atoms by collisions with the H_2 molecules of the gas target and from possible transitions in exotic hydrogen molecules. The instrumental response is being studied using a transition in helium-like ions[43], emitted by the plasma of an Electron-Cyclotron Ion Trap (ECRIT) build at PSI[44]. High-intensity spectra, allow for systematic study of instrumental response. Exotic atoms do not provide as good a response function calibration as most line coming from molecules are broadened by Doppler effect due to the Coulomb explosion during the atom formation process [45], and as the rate being much lower, the statistic is often not sufficient. An example of an highly-charged argon spectrum in the energy range of interest is presented on Fig. 6.

4 Antiprotonic atoms

The operation of LEAR, a low-energy antiproton storage ring with stochastic and electron cooling at CERN from 1983 to 1996 has caused a real revolution in antiproton physics. Numerous particle physics experiments were conducted there, but also atomic physics experiments. A number of the latter used antiprotonic atoms produced with the cyclotron trap (from $\bar{p}H$ to $\bar{p}Xe$). Others used Penning trap to measure the antiproton/proton mass ratio to test CPT invariance [46]. An other experiment was concerned with precision laser spectroscopy of metastable states of the $He^+\bar{p}$ system [47], the existence of which had been discovered earlier at KEK [48]. This experiment is now being continued with improved accuracy at LEAR successor, the

AD (Antiproton Decelerator). Compared with recent high-accuracy three-body calculations with relativistic and QED corrections, these experiments provide very good upper bounds to the charge and mass differences between proton and antiproton, again testing CPT invariance[49]. More recently the hyperfine structure of the ${}^3\text{He}^+\bar{p}$ atoms as been investigated [50] and found in good agreement with theory [51]. Expected accuracy improvements in the new AD experiment ASACUSA, should lead to even more interesting results [52].

4.1 Antiprotonic hydrogen and deuterium

X-ray spectroscopy of antiprotonic hydrogen and deuterium was performed at LEAR to study the strong interaction between nucleon and antinucleon at low energy. First the use of solid state detectors like Si-Li detectors, provided some information. The study of line intensities provided estimates of the antiproton annihilation in the 2p state. The 2p \rightarrow 1s transitions were observed. While the transition energy is around 8.7 keV, the 1s broadening due to annihilation is 1054 ± 65 eV and the strong interaction shift is -712.5 ± 25.3 eV. Measuring such a broad line is very difficult as many narrow contamination lines will be superimposed on it. Moreover those rather precise values are spin-averaged quantities that neglect the unknown 1s level splitting. More recently the use of CCD detectors has allowed to improve the $\bar{p}\text{H}$ measurement [53] and to make the first observation of $\bar{p}\text{D}$ line, which is even broader, due to three body effects [54].

The broadening of the 2p state however is much smaller. The Balmer 3d \rightarrow 2p lines can thus be studied by crystal spectroscopy. The use of the cyclotron trap allowing to capture antiprotons in dilute gases with a 90 % efficiency and of an efficient, high-resolution crystal spectrometer were instrumental to the success of such an experiment, owing to the low production rate of antiprotons (a few 10^8 per hour). With that a counting rate of around 25 counts per hour was observed, due to the use of an ultimate resolution device, even optimized for efficiency. The experimental set-up is basically the same as described in Sec. 3. However to improve X-ray collection efficiency, a double spectrometer was build, with two arms symmetrical with respect to the trap axis and three crystals. On one side a large CCD detector allowed to have two vertically super-imposed crystals. On the other side a single crystal was mounted. Resolutions of around 290 meV where achieved, which are of the order of the expected line splitting. The final spectrum observed with one of the three crystal/detector combination is presented on Fig. 7.

In order to extract strong interaction parameters from such spectrum, a detailed description of the QED structure of the multiplet is required. Antiproton being composed of three quarks are not point-like, Dirac particles. In particular their gyro-magnetic ratio is very different : for the antiproton we have $a_{\bar{p}} = (g - 2)/2 = -1.792847386$ instead of $-\alpha/(2\pi) \approx -1.2 \times 10^{-3}$ for a positron. The corrections due to the anomalous magnetic moment of the antiproton can be accounted for by introducing the operator (valid for distances larger than the Compton wavelength of the electron \hbar/mc)

$$\Delta H = a \frac{\hbar q}{2m_p} \beta \left(i \frac{\boldsymbol{\alpha} \mathbf{E}}{c} - \boldsymbol{\Sigma} \mathbf{B} \right), \quad (2)$$

where m_p is the antiproton mass, \mathbf{E} and \mathbf{B} are the electric and magnetic fields generated by the nucleus, $\boldsymbol{\alpha}$ are Dirac matrices and

$$\boldsymbol{\Sigma} = \begin{pmatrix} \boldsymbol{\sigma} & 0 \\ 0 & \boldsymbol{\sigma} \end{pmatrix}. \quad (3)$$

Vacuum polarization corrections and finite particle size (both for the nucleus and the antiproton) must be included. Because the antiproton is ≈ 2000 times closer to the nucleus than in the hydrogen case, hyperfine structure and the $g - 2$ correction are very large, even larger than the fine structure. In such a case perturbation theory is insufficient to account for the effect. The full Hamiltonian matrix over the 2p and 3d Dirac states must be build and diagonalized. The result of such a fully relativistic calculation for antiprotonic deuterium is shown in Fig. 8, together with the result of earlier calculation [55]. The large difference between the two results is not understood. However the results from [55] do not reproduce correctly the observed line shape [56]. By combining the high-precision measurements carried out with the cyclotron trap and the spherical crystal spectrometer, and the theoretical calculations presented above, it has been possible to evaluate strong interaction shifts for the 2p level, and different $\bar{p}H$ and $\bar{p}D$ spin states [56]. The results confirm calculations based on the Dover-Richard semi-phenomenological potential [57, 58] (see [56] for more details).

5 Conclusion and perspectives

In this paper, I have explored different aspects of the physics of light muonic, pionic and antiprotonic atoms. I have left out many aspects of that physics, like the study of the atomic cascade, collisions between exotic atoms and gases, or the atomic and molecular phenomena involved in muon-catalyzed fusion. The formation of antiprotonic highly-charged ions as has been observed at LEAR seems to point to very exciting new atomic physics[59]. I have not explored either the studies of interest to nuclear physics like measurement of nuclear charge distribution for heavier elements with muonic atoms (see, e.g., [60]) or of neutron distribution with antiprotonic atoms[61]. With the continuous progress in accelerators technology (improvements in the intensity at PSI), the development of very low energy antiproton energy at the AD at CERN, the trapping of antihydrogen[62, 63], or the new antiproton machine at GSI, it is expected that this physics will continue to develop in the years to come and provide more challenges to atomic and fundamental physics.

Acknowledgments Laboratoire Kastler Brossel is Unité Mixte de Recherche du CNRS n° C8552. I wish to thank all the participants to the antiprotonic hydrogen, pion mass, pionic hydrogen and muonic hydrogen experiments for their relentless effort to make those experiments live and develop. I am in particular indebted to D. Gotta, L. Simons, F. Kottmann and F. Nez. On the theoretical side, participation of S. Boucard, V. Yerokhin, E.O. Le Bigot, V. Shabaev and P.J. Mohr is gratefully acknowledged.

References

- [1] G. S. Adkins, R. N. Fell, and J. Sapirstein, *Ann. Phys. (N.Y.)* **295**, 136 (2002).
- [2] R. Vallery, P. Zitzewitz, and D. Gidley, *Phys. Rev. Lett.* **90**, 203402 (4) (2003).
- [3] M. Fee, S. Chu, J. A.P. Mills, R. Chichester, D. Zuckerman, E. Shaw, and K. Danzmann, *Phys. Rev. A* **48**, 192 (1993).
- [4] V. W. Hughes, *Z. Phys. C* **56**, S35 (1992).

- [5] W. Liu, M. G. Boshier, S. Dhawan, O. v. Dyck, P. Egan, X. Fei, M. Grosse Perdekamp, V. W. Hughes, M. Janousch, K. Jungmann, et al., *Phys. Rev. Lett.* **82**, 711 (1999).
- [6] S. Chu, A. P. Mills Jr, A. G. Yodh, K. Nagamine, Y. Miyake, and T. Kuga, *Phys. Rev. Lett.* **60**, 101 (1988).
- [7] K. Danzmann, M. S. Fee, and S. Chu, *Phys. Rev. A* **39**, 6072 (1989).
- [8] W. Schwarz, P. E. G. Baird, J. R. M. Barr, D. Berkeland, M. G. Boshier, B. Braun, G. H. Eaton, A. I. Ferguson, H. Geerds, V. W. Hughes, et al., *IEEE Transac. Instrum. Measur.* **44**, 505 (1995).
- [9] V. Meyer, S. N. Bagayev, P. E. G. Baird, P. Bakule, M. G. Boshier, A. Breitrück, S. L. Cornish, S. Dychkov, G. H. Eaton, A. Grossmann, et al., *Phys. Rev. Lett.* **84**, 1136 (2000).
- [10] K. Melnikov and A. Yelkhovsky, *Phys. Rev. Lett.* **86**, 1498 (2001).
- [11] R. J. Hill, *Phys. Rev. Lett.* **84**, 3280 (2001).
- [12] M. I. Eides, H. Grotch, and V. A. Shelyuto, *Phys. Rep.* **342**, 63 (2001).
- [13] P. J. Mohr and B. N. Taylor, *Rev. Mod. Phys.* **72**, 351 (2000).
- [14] L. M. Simons, D. Abbot, B. Bach, R. Bacher, A. Badertscher, P. Blüm, P. DeCecco, J. Eades, J. Egger, K. Elsener, et al., *Nucl. Instrum. Methods B* **87**, 293 (1994).
- [15] M. Niering, R. Holzwarth, J. Reichert, P. Pokasov, T. Udem, M. Weitz, T. W. Hänsch, P. Lemonde, G. Santarelli, M. Abgrall, et al., *Phys. Rev. Lett.* **84**, 5496 (2000).
- [16] B. de Beauvoir, C. Schwob, O. Acef, L. Jozefowski, L. Hilico, F. Nez, L. Julien, A. Clairon, and F. Biraben, *Eur. Phys. J. D* **12**, 61 (2000).
- [17] S. Mallampalli and J. Sapirstein, *Phys. Rev. A* **57**, 1548 (1998).
- [18] S. Mallampalli and J. Sapirstein, *Phys. Rev. Lett.* **80**, 5297 (1998).
- [19] V. A. Yerokhin, *Phys. Rev. A* **62**, 012508 (2000).
- [20] V. Yerokhin, P. Indelicato, and V. Shabaev, *Phys. Rev. Lett.* **91**, in press (2003).
- [21] L. Hand, D. T. Miller, and R. Willson, *Rev. Mod. Phys.* **35**, 335 (1963).
- [22] P. Mergell, U. Meissner, and D. Drechsel, *Nucl. Phys. A* **596**, 367 (1996).
- [23] R. Rosenfelder, *Phys. Lett. B* **479**, 381 (2000).
- [24] G. G. Simon, C. Schmidt, F. Borkowski, and V. H. Walther, *Nucl. Phys. A* **333**, 381 (1980).
- [25] K. Pachucki, *Phys. Rev. A* **53**, 2092 (1996).
- [26] K. Pachucki, *Phys. Rev. A* **60**, 3593 (1999).

- [27] L. Simons, *Hyp. Int.* **81**, 253 (1993).
- [28] P. DeCecco, P. Hauser, D. Horvath, F. Kottmann, J. Missimer, L. M. Simons, D. Taqqu, D. Abbot, B. Bach, R. T. Siegel, et al., *Hyp. Int.* **76**, 275 (1993).
- [29] D. Taqqu, *Hyp. Int.* **101/102**, 633 (1996).
- [30] D. Taqqu, F. Biraben, C. A. N. Conde, T. W. Hänsch, F. J. Hartmann, P. Hauser, P. Indelicato, P. Knowles, F. Kottmann, F. Mulhauser, et al., *Hyp. Int.* **119**, 311 (1999).
- [31] R. Pohl, F. Biraben, C. A. N. Conde, C. Donche Gay, T. W. Hänsch, F. J. Hartmann, P. Hauser, V. W. Hughes, O. Huot, P. Indelicato, et al., *Hyp. Int.* **127**, 161 (2000).
- [32] F. Kottmann, W. Amir, F. Biraben, C. A. N. Conde, S. Dhawan, T. W. Hänsch, F. J. Hartmann, V. W. Hughes, O. Huot, P. Indelicato, et al., *Hyp. Int.* **138**, 55 (2001).
- [33] B. Jeckelmann, T. Nakada, W. Beer, G. de Chambrier, O. Elsenhans, K. L. Giovanetti, P. F. A. Goudsmit, H. J. Leisi, A. Ruetschi, O. Piller, et al., *Phys. Rev. Lett.* **56**, 1444 (1986).
- [34] B. Jeckelmann, W. Beer, G. De Chambrier, O. Elsenhans, K. Giovanetti, P. Goudsmit, H. Leisi, T. Nakada, O. Piller, A. Ruetschi, et al., *Nucl. Phys. A* **457**, 709 (1986).
- [35] K. Assamagan, C. Brönnimann, M. Daum, H. Forrer, R. Frosch, P. Gheno, R. Horisberger, M. Janousch, P. Kettle, T. Spirig, et al., *Physics Letters B* **335**, 231 (1994).
- [36] S. Lenz, G. Borchert, H. Gorke, D. Gotta, T. Siems, D. Anagnostopoulos, M. Augsburg, D. Chatellard, J. Egger, D. Belmiloud, et al., *Physics Letters B* **416**, 50 (1998).
- [37] N. Nelms, D. F. Anagnostopoulos, O. Ayranov, G. Borchert, J. P. Egger, D. Gotta, M. Hennebach, P. Indelicato, B. Leoni, Y. W. Liu, et al., *Nucl. Instrum. Meth. A* **484**, 419 (2002).
- [38] N. Nelms, D. F. Anagnostopoulos, M. Augsburg, G. Borchert, D. Chatellard, M. Daum, J. P. Egger, D. Gotta, P. Hauser, P. Indelicato, et al., *Nucl. Instr. Meth.* **477**, 461 (2002).
- [39] S. Boucard, P. Patté, and P. Indelicato (2002), to be published.
- [40] S. Weinberg, *Phys. Rev. Lett.* **17**, 616 (1966).
- [41] S. Deser, M. L. Goldberger, K. Baumann, and W. Thirring, *Phys. Rev.* **96**, 774 (1954).
- [42] P. Hauser, K. Kirch, L. Simons, G. Borchert, D. Gotta, T. Siems, P. El-Khoury, P. Indelicato, M. Augsburg, D. Chatellard, et al., *Phys. Rev. C* **58**, R1869 (1998).
- [43] D. F. Anagnostopoulos, S. Biri, V. Boisbourdain, M. Demeter, G. Borchert, J. P. Egger, H. Fuhrmann, D. Gotta, A. Gruber, M. Hennebach, et al., *Nucl. Instrum. Methods B* **205**, 9 (2003).
- [44] S. Biri, L. Simons, and D. Hitz, *Review of Scientific Instruments* **71**, 1116 (2000).

- [45] T. Siems, D. Anagnostopoulos, G. Borchert, D. Gotta, P. Hauser, K. Kirch, L. Simons, P. El-Khoury, P. Indelicato, M. Augsburger, et al., Phys. Rev. Lett. **84**, 4573 (2000).
- [46] G. Gabrielse, A. Khabbaz, D. S. Hall, C. Heimann, H. Kalinowsky, and W. Jhe, Phys. Rev. Lett. **82**, 3198 (1999).
- [47] R. Hayano, F. Maas, H. Torii, N. Morita, M. Kamakura, T. Yamazaki, H. Masuda, I. Sugai, F. Hartmann, H. Daniel, et al., Phys. Rev. Lett. **73**, 1485 (1994).
- [48] M. Iwasaki, S. N. Nakamura, K. Shigaki, Y. Shimizu, H. Tamura, T. Ishikawa, R. S. Hayano, E. Takada, E. Widmann, H. Outa, et al., Phys. Rev. Lett. **67**, 1246 (1991).
- [49] M. Hori, J. Eades, R. S. Hayano, T. Ishikawa, J. Sakaguchi, E. Widmann, H. Yamaguchi, H. A. Torii, B. Juhász, D. Horváth, et al., Phys. Rev. Lett. **87**, 093401 (2001).
- [50] E. Widmann, J. Eades, T. Ishikawa, J. Sakaguchi, T. Tasaki, H. Yamaguchi, R. S. Hayano, M. Hori, H. A. Torii, B. Juhász, et al., Phys. Rev. Lett. **89**, 243402 (2002).
- [51] D. Bakalov and V. Korobov, Phys. Rev. A **57**, 1662 (1998).
- [52] T. Yamazaki, N. Morita, R. S. Hayano, E. Widmann, and J. Eades, Phys. Rep. **266**, 183 (2002).
- [53] M. Augsburger, D. Anagnostopoulos, G. Borchert, D. Chatellard, J. Egger, P. El-Khoury, H. Gorke, D. Gotta, P. Hauser, P. Indelicato, et al., Nucl. Phys. A **658**, 149 (1999).
- [54] M. Augsburger, D. Anagnostopoulos, G. Borchert, D. Chatellard, J.-P. Egger, P. El-Khoury, H. Gorke, D. Gotta, P. Hauser, P. Indelicato, et al., Phys. Lett. B **461**, 417 (1999).
- [55] S. Barmo, H. Pilkuhn, and H. Schlaile, Z. Phys. A **301**, 283 (1981).
- [56] D. Gotta, D. F. Anagnostopoulos, M. Augsburger, G. Borchert, C. Castelli, D. Chatellard, J. P. Egger, P. El-Khoury, H. Gorke, P. Hauser, et al., Nucl. Phys. A **660**, 283 (1999).
- [57] C. Dover and J. Richard, Phys. Rev. C **21**, 1466 (1980).
- [58] J. Richard and M. Sainio, Physics Letters B **110**, 349 (1982).
- [59] K. Rashid, D. Gotta, B. Fricke, I. P., and L. Simons, *Antiprotonic and electronic transitions in noble gases*, private comm.
- [60] C. Batty, E. Friedman, H. Gils, and H. Rebel, in *Advances in Nuclear Physics*, edited by J. Negele and E. Vogt (Plenum, New-York, 1989), vol. 19, pp. 1–188.
- [61] A. Trzcinska, J. Jastrzebski, P. Lubiski, F. J. Hartmann, R. Schmidt, T. von Egidy, and B. Klos, Phys. Rev. Lett. **87**, 082501 (4) (2001).
- [62] M. Amoretti, C. Amsler, G. Bonomi, A. Bouchta, P. Bowek, C. Carraro, C. Cesar, M. Charlton, M. Collier, M. Doserà, et al., Nature **419**, 456 (2002).

- [63] G. Gabrielse, N. S. Bowden, P. Oxley, A. Speck, C. H. Storry, J. N. Tan, M. Wessels, D. Grzonka, W. Oelert, G. Schepers, et al., *Phys. Rev. Lett.* **89**, 233401 (2002).

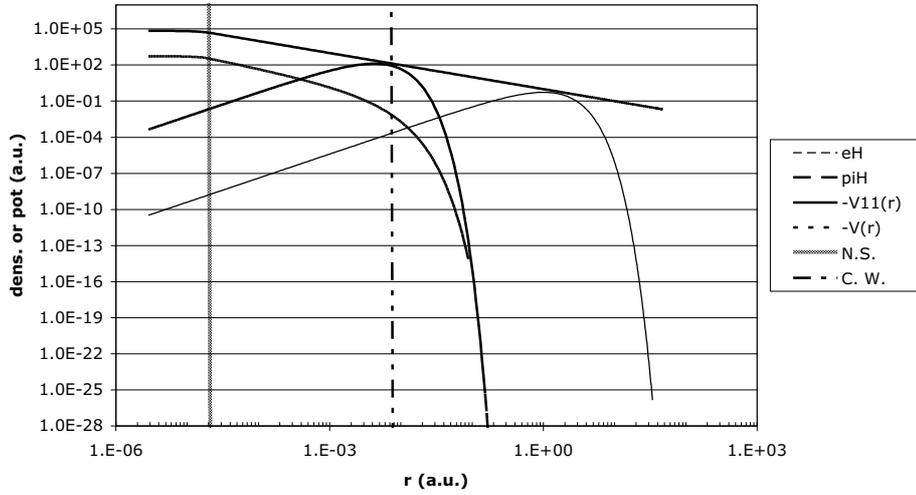


Figure 1: Natural scales comparison in pionic and normal hydrogen. C.W.: compton wavelength of the electron (QED scale). N.S.: proton radius (strong interaction scale). eH: hydrogen 1s electronic density. piH: pionic hydrogen 1s density. -V11: Uelhing (vacuum polarization) potential. V: Coulomb potential

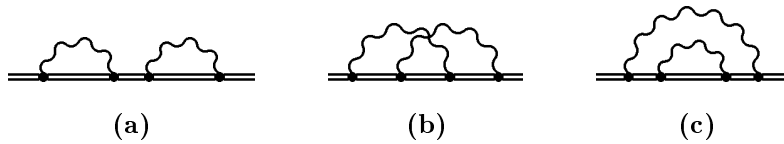


Figure 2: The three Feynman diagrams contributing to the two-loop self-energy. Double lines represent bound electron propagators and wavy lines photon propagators. Diagram (a) represents the loop-after-loop term. The irreducible part is obtained when the propagator between the two-loop has an energy different from the energy of the bound state being studied [20].

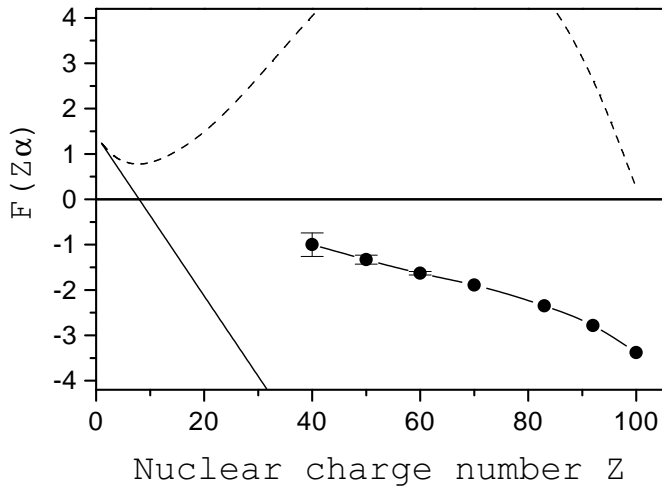


Figure 3: Comparison with all-order numerical calculation and the function obtained from the first or second order expansion in $Z\alpha$.

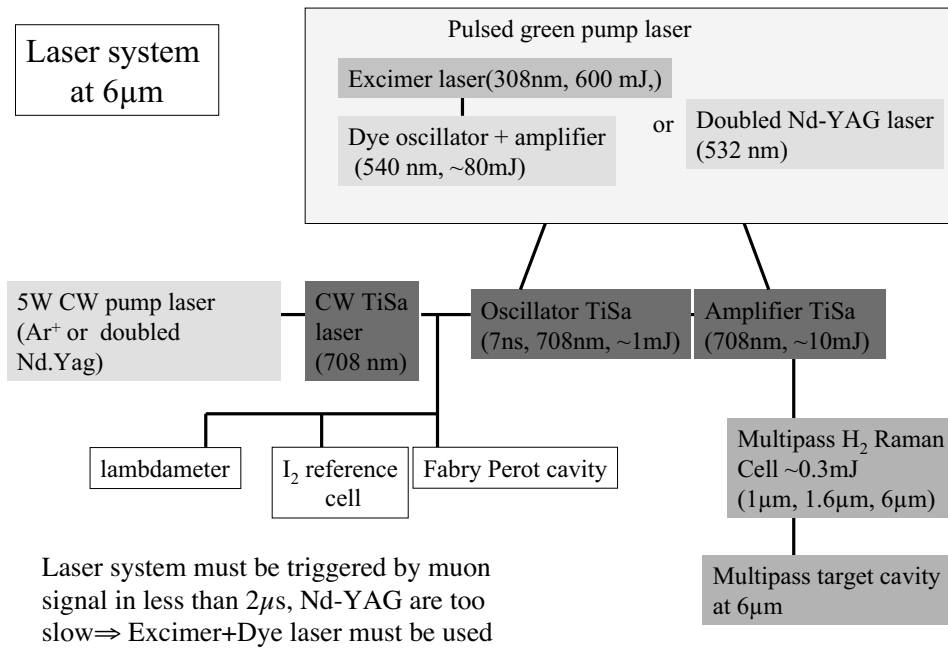


Figure 4: Principle of the $6\mu\text{m}$ laser for the study of the muonic hydrogen $2s \rightarrow 2p$ transition

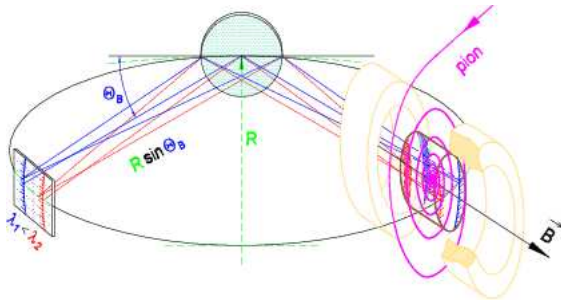


Figure 5: Principle of X-ray spectroscopy of exotic atoms with the cyclotron trap and a spherically curved crystal spectrometer. The bidimensional X-ray detector is a 6-chips cooled CCD detector and is located on the Rowland circle of radius $R/2$, where R is the radius of curvature of the crystal (≈ 3 m)

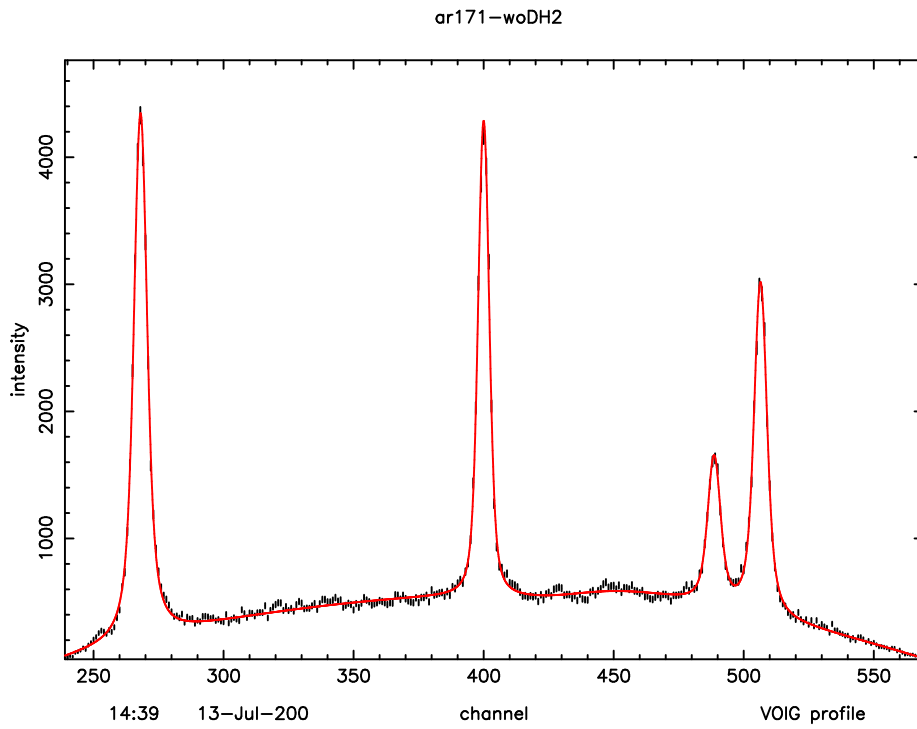


Figure 6: High-statistic X-ray spectrum from the $1s2s^3S_1 \rightarrow 1s^2^1S_0$ transition in helium-like argon (center line) from the PSI Electron-Cyclotron Resonance Ion Trap. 37500 counts were accumulated in this line in 35 min, using the instrument in Fig. 5. The width of this 3.1 keV line is 0.4 eV. The line on the left is from Ar^{14+} and those on the right are from Ar^{15+} .

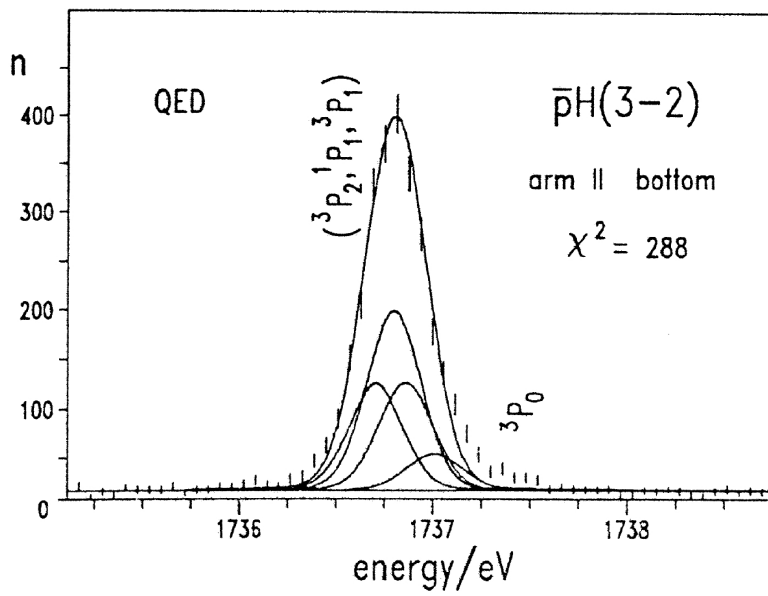


Figure 7: High-resolution spectrum of antiprotonic hydrogen [56]. The difference between the measured line shape and the solid line is due to the fact that the solid line represents a line-shape model without strong interaction, evaluated following the method described in the text (2).

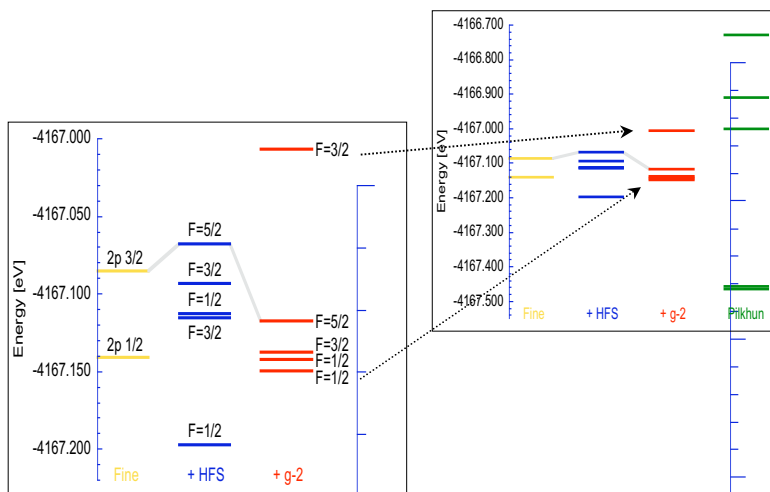


Figure 8: Theoretical level scheme of antiprotonic deuterium and comparison with earlier work (Pilkuhn) [55].